Electromagnetic Imaging for an Imperfectly Conducting Cylinder by the Genetic Algorithm

Chien-Ching Chiu and Wei-Ting Chen

***Abstract*—This paper presents a computational approach to the imaging of an imperfectly conducting cylinder by the genetic algorithm (GA). A conducting cylinder of unknown shape and conductivity scatters the incident wave in free space and the scattered field is recorded outside. Based on the boundary condition and the measured scattered field, a set of nonlinear integral equations is derived and the imaging problem is reformulated into an optimization problem. The GA is then employed to find out the global extreme solution of the cost function. Numerical results demonstrated that, even when the initial guess is far away from the exact one, good reconstruction has been obtained. In such a case, the gradient-based methods often get trapped in a local extreme. In addition, the effect of Gaussian noise on the reconstruction results is investigated. Numerical results show that multiple incident directions permit good reconstruction of shape and, to a lesser extent, conductivity in the presence of noise in measured data.**

***Index Terms*—Conductors, electromagnetic scattering inverse problems, genetic algorithms, image reconstruction.**

I. Introduction

THE image problem of conducting objects has been a subject of considerable importance in noninvasive measurement, medical imaging, and biological application. In the past 20 years, many rigorous methods have been developed to solve the exact equation. However, inverse problems of this type are difficult to solve because they are ill posed and nonlinear. As a result, many inverse problems are reformulated as optimization problems. Generally speaking, two main kinds of approaches have been developed. The first is based on gradient search approach such as the Newton–Kantorovitch method [1]–[3], local shape function method [4], Levenberg–Marguart algorithm [5]–[7], and successive-overrelaxation method [8] since these approaches apply the gradient search method to find the extreme of the cost function. This method is highly dependent on the initial guess and tends to get trapped in a local extreme. In contrast, the second approach is based on the genetic algorithm (GA) [9]–[11]. The GA is a well-known algorithm that uses the stochastic random choice to search through a coding of a parameter space. Compared to gradient search optimization techniques, the GA is less prone to convergence to a local minimum, which, in turn, renders it an ideal candidate for global optimization. It usually converges to the global extreme of the problem, no matter what the initial estimate is [12]. However, the aforementioned GA merely deals with the case of perfectly conducting objects, and there is still no research for the case involving lossy or imperfect metallic scatterers.

In this paper, the electromagnetic imaging of an imperfectly conducting (i.e., lossy) cylinder in free space is investigated. The GA is used to recover not only the shape, but also the conductivity, of a scatterer by using only the scattered field. The method is potentially important in medical imaging and biological application. In Section II, a theoretical formulation for the electromagnetic imaging is presented. The general principle of GAs and the way we applied them to the imaging problem are described. Numerical results for objects of different shapes and conductivities are given in Section III. Finally, some conclusions are drawn in Section IV.

Manuscript received January 4, 2000; revised March 21, 2000. This work was supported by the National Science Council, R.O.C. under Grant NSC-87-2213-E-032-022.

The authors are with the Electrical Engineering Department, Tamkang University, 25137 Taiwan, R.O.C.

Publisher Item Identifier S 0018-9480(00)09980-4.

II. Theoretical Formulation

A. Imaging Problem

Let us consider an imperfectly conducting cylinder with conductivity σ located in free space, and let (ε_0, μ_0) denote the permittivity and permeability, respectively, of free space. The metallic cylinder with a cross section described in polar coordinates in the xy-plane by $\rho = F(\theta)$ is illuminated by an incident plane wave whose electric-field vector is parallel to the Z–axis (i.e., TM polarization). Let $\vec{E}_i$ denote the incident plane wave with an incident angle ϕ, as shown in Fig. 1. The scattered field $\vec{E}_s = \vec{E} - \vec{E}_i$ can then be expressed by

$$E_s(x, y) = -\int_0^{2\pi} \frac{j}{4} H_0^{(2)} \cdot \left(k\sqrt{(x - F(\theta')\cos(\theta'))^2 + (y - F(\theta')\sin(\theta'))^2}\right) \cdot J(\theta')\, d\theta' \quad (1)$$

with

$$J(\theta) = -j\omega\mu_0\sqrt{F^2(\theta) + F'^2(\theta)}J_s(\theta), \quad k^2 = \omega^2\varepsilon_0\mu_0$$

where $H_0^{(2)}$ is the Hankel function of the second kind of order zero, and $J_s(\theta)$ is the induced surface current density. The boundary condition for an imperfectly conducting scatterer with finite conductivity can be approximated by assuming that the total tangential electric field on the scatterer surface is related to surface current density through a surface impedance

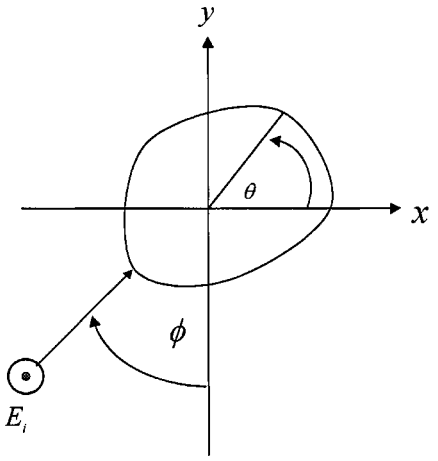

Fig. 1. Geometry of the problem in the (x, y)-plane.

[3], [13], [14]. This boundary condition yields an integral equation for $J(\theta)$

$$E_i(F(\theta), \theta) = \int_0^{2\pi} \frac{j}{4} H_0^{(2)}(kr_0) J(\theta')\, d\theta' + j\sqrt{\frac{j}{\omega\mu_0\sigma}} \frac{J(\theta)}{\sqrt{F^2(\theta) + F'^2(\theta)}} \quad (2)$$

where

$$r_0(\theta, \theta') = \left[F^2(\theta) + F^2(\theta') - 2F(\theta)F(\theta')\cos(\theta - \theta')\right]^{1/2}.$$

For the direct scattering problem, the scattered field E_s is calculated by assuming that the shape and conductivity of the object are known. This can be achieved by first solving J in (2) and calculating E_s in (1). For numerical calculation of the direct problem, the contour is first divided into sufficiently small segments so that the induced surface current density can be considered constant over each segment. The moment method [15] is then used to solve (1) and (2) with a pulse basis function for expanding and the Dirac delta function for testing.

Let us consider the following inverse problem: given the scattered field E_s measured outside the scatterer, determine the shape $F(\theta)$ and conductivity σ of the object. Assume the approximate center of the scatterer (which, in fact, can be any point inside the scatterer) is known. The shape $F(\theta)$ function can then be expanded as

$$F(\theta) = \sum_{n=0}^{N/2} B_n \cos(n\theta) + \sum_{n=1}^{N/2} C_n \sin(n\theta) \quad (3)$$

where B_n and C_n are real coefficient to be determined, and $N + 1$ is the number of unknowns for shape function. In the inversion procedure, the GA is used to minimize the following cost function:

$$CF = \left\{ \frac{1}{M_t} \sum_{m=1}^{M_t} |E_s^{\exp}(\vec{r}_m) - E_s^{\text{cal}}(\vec{r}_m)|^2 \Big/ |E_s^{\exp}(\vec{r}_m)|^2 + \alpha |F'(\theta)|^2 \right\}^{1/2} \quad (4)$$

where M_t is the total number of measured points. $E_s^{\exp}(\vec{r})$ and $E_s^{\text{cal}}(\vec{r})$ are the measured and calculated scattered fields, respectively. Note that the regularization term $\alpha|F'(\theta)|^2$ was added in (4). Please refer to [3] and [9] for further detail.

B. Genetic Algorithm

Genetic algorithms are the global numerical optimization methods based on genetic recombination and evolution in nature [12]. They use the iterative optimization procedures that start with a randomly selected population of potential solutions, and then gradually evolve toward a better solution through the application of the genetic operators, i.e., reproduction, crossover, and mutation operators. In our problem, both parameters B_n and C_n are coded by the following equation:

$$B_n(\text{or } C_n) = p_{\min} + \frac{p_{\max} - p_{\min}}{2^L - 1} \sum_{i=0}^{L-1} b_i^{B_n(\text{or } C_n)} 2^i \quad (5)$$

$$\sigma = q_{\min} + \frac{q_{\max} - q_{\min}}{2^{N_I} - 1} \sum_{i=1}^{N_i - 1} d_i 2^i. \quad (6)$$

The $b_0^{B_n(\text{or } C_n)}, b_1^{B_n(\text{or } C_n)}, \ldots, b_{L-1}^{B_n(\text{or } C_n)}$ (gene) is the L-bit string of the binary representation of B_n (or C_n), and $p_{\min}$ and $p_{\max}$ are the minimum and maximum values admissible for B_n (or C_n), respectively. Similarly, $d_0, d_1, \ldots, d_{N_I-1}$ is the N_I-bit string of the binary representation of σ, and $q_{\min}$ and $q_{\max}$ are the minimum and maximum values admissible for σ, respectively. Here, $p_{\min}$, $p_{\max}$, $q_{\min}$, and $q_{\max}$ can be determined by prior knowledge of the object. Also, the finite resolution with which B_n (or C_n), σ can be tuned in practice is reflected in the number of bits assigned to it. The total unknown coefficients in (3), (5), and (6) would then be described by an $(N+1)\times L + N_I$ bit string (chromosome). The basic GA for which a flowchart is shown in Fig. 2 starts with a large population containing a total of M candidates. Each candidate is described by a chromosome. The initial population can then simply be created by taking M random chromosomes. Finally, the GA iteratively generates a new population, which is derived from the previous population through the application of the reproduction, crossover, and mutation operators. The new populations will contain increasingly better chromosomes and will eventually converge to an optimal population that consists of the optimal chromosomes. As soon as the cost function (CF) changes by $<1\%$ in two successive generations, the algorithm will be terminated and a solution is then obtained.

III. Numerical Results

By numerical simulation, we illustrate the performance of the proposed inversion algorithm and its sensitivity to random error in the scattered field. Let us consider an imperfectly conducting cylinder in free space and a plane wave of unit amplitude incident upon the object, as shown in Fig. 1. The frequency of the incident wave is chosen to be 3 GHz, i.e., the wavelength λ is 0.1 m. In the examples, the size of the scatterer is about one-third the wavelength, thus, the frequency is in the resonance range.

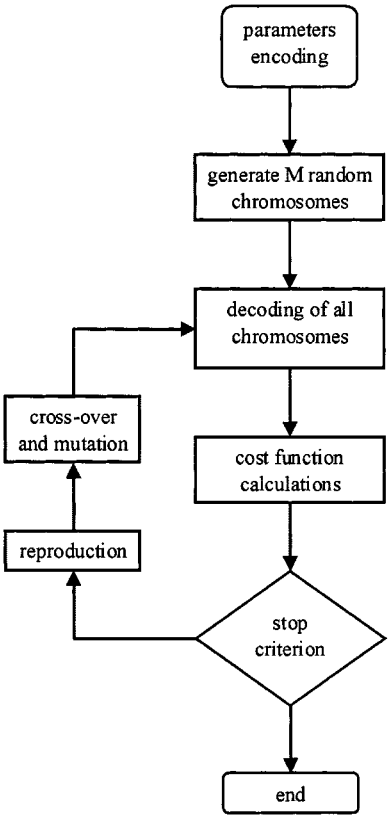

Fig. 2. Flowchart for the GA.

In our calculation, three examples are considered. To reconstruct the shape and conductivity of the cylinder, the object is illuminated by four incident waves with incident angles $\phi = 0°$, $90°$, $180°$, and $270°$, and the measurement is taken on a circle of radius R' at equal spacing. In our cases, R' is chosen much larger than $2D'^2/\lambda$, corresponding to the far-field measurement, where D' is the largest dimension of the scatterer. Note that for each incident angle, eight measurement points at equal spacing are used, and there are a total of 32 measurement points in each simulation. The number of unknowns is set to ten (i.e., $N + 2 = 10$) to save computing time. The population size is chosen as 300 (i.e., $M = 300$). The binary string length of unknown coefficient B_n (or C_n) is set to be 16 bits (i.e., $L = 16$). The binary string length of conductivity σ is also set to be 16 bits (i.e., $N_I = 16$). In other words, the bit number of a chromosome is 160 bits. The search range for unknown coefficient of the shape function is chosen to be from 0 to 0.1. The search range for unknown conductivity is chosen from 3×10^7 to 7×10^7. The extreme value of the coefficient of the shape function and conductivity can be determined by the prior knowledge of the objects. The crossover probability p_c and mutation probability p_m are set to be 0.8 and 0.04, respectively. The value of α is chosen to be 0.001.

In the first example, the shape function is chosen to be $F(\theta) = (0.03 + 0.0025\cos\theta - 0.005\cos 2\theta + 0.005\cos 3\theta)$ m with aluminum material (i.e., $\sigma = 3.54 \times 10^7$ s/m). The reconstructed shape function for the best population member (chromosome) is plotted in Fig. 3(a) with the error shown in Fig. 3(b), while the error for the reconstructed conductivity is also given in Fig. 3(b). Here, DR and DSIG, which are the

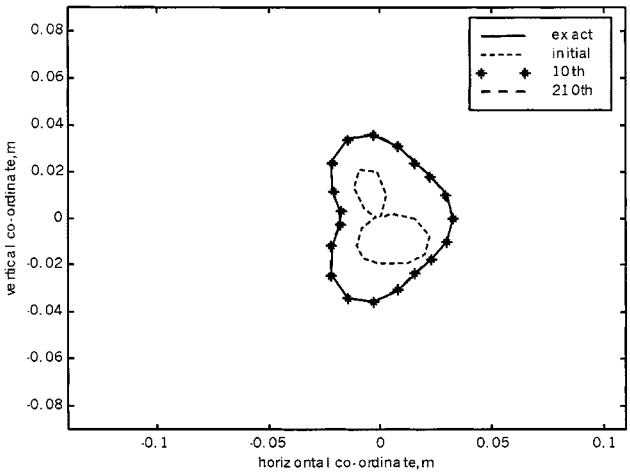

(a)

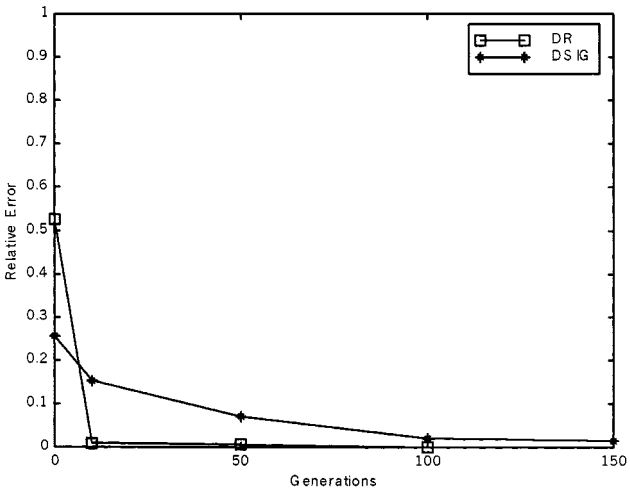

(b)

Fig. 3. (a) Shape function for example 1. The solid curve represents the exact shape, while the dashed curves are calculated shape in iteration process. (b) Shape-function error and conductivity error in each generation.

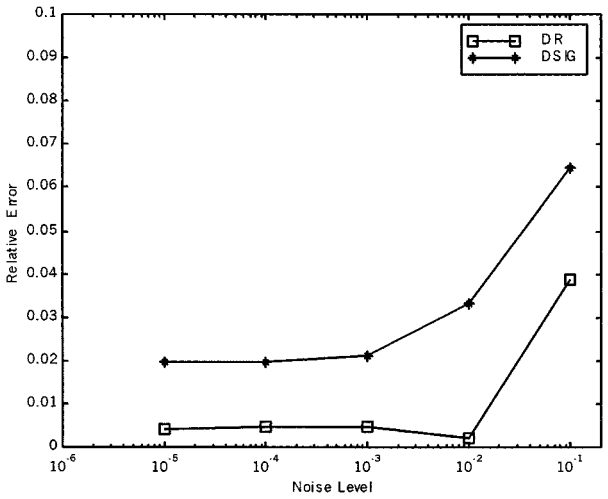

Fig. 4. Relative error of shape and conductivity as a function of noise.

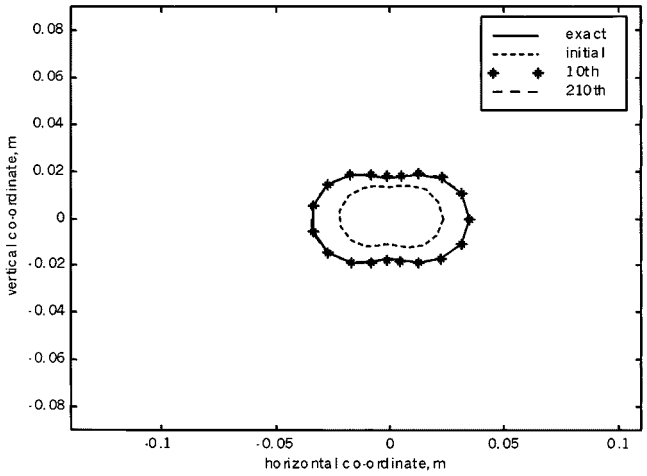

(a)

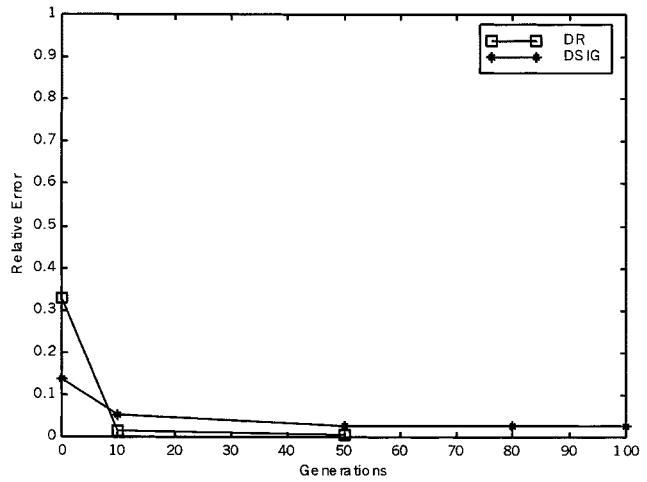

(b)

Fig. 5. (a) Shape function for example 2. The solid curve represents the exact shape, while the dashed curves are the calculated shape in the iteration process. (b) Shape function error and conductivity error in each generation.

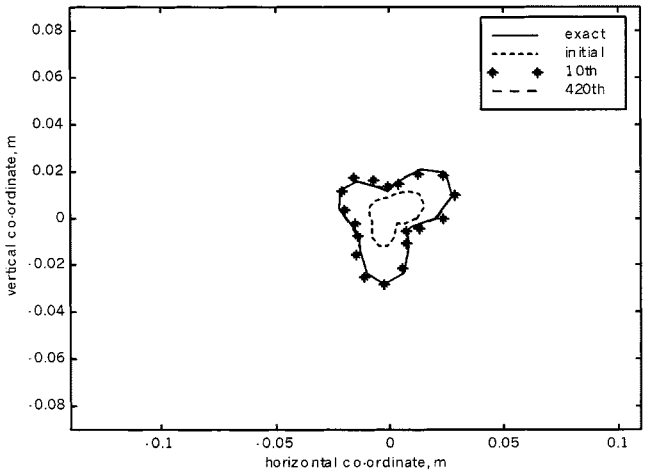

(a)

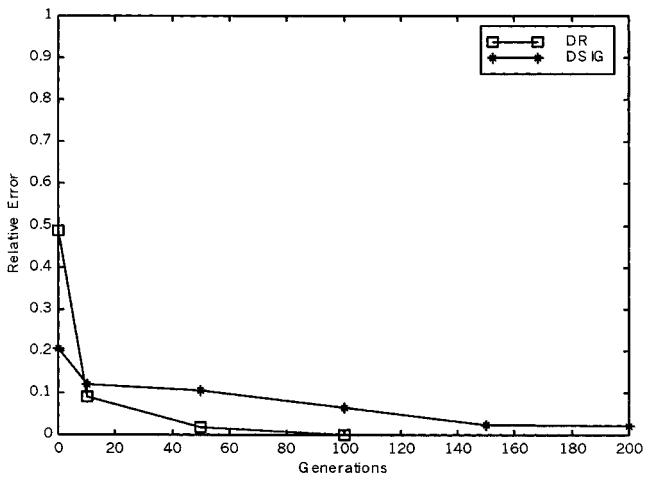

(b)

Fig. 6. (a) Shape function for example 3. The solid curve represents the exact shape, while the dashed curves are the calculated shape in the iteration process. (b) Shape function error and conductivity error in each generation.

shape function and conductivity discrepancies, respectively, are defined as

$$\mathrm{DR} = \left\{ \frac{1}{N'} \sum_{i=1}^{N'} [F^{\mathrm{cal}}(\theta_i) - F(\theta_i)]^2 \Big/ F^2(\theta_i) \right\}^{1/2}$$

$$\mathrm{DSIG} = \left| \frac{\sigma^{\mathrm{cal}} - \sigma}{\sigma} \right|$$

where N' is set to 60. The quantities DR and DSIG provide measures of how well F^{cal} approximate $F(\theta)$ and σ^{cal} approximates σ, respectively. From Fig. 3, it is clear that the reconstruction of the shape function and conductivity is quite good. The quantity DSIG is 1.7×10^{-2} in the final generation. In addition, we also see that the reconstruction of conductivity does not change rapidly toward the exact value until DR is small enough. This can be explained by the fact that the shape function makes a stronger contribution to the scattered field than the conductivity does. In other words, the reconstruction of the shape function has a higher priority than the reconstruction of the conductivity. To investigate the sensitivity of the imaging algorithm against random noise, two independent Gaussian noises with zero mean have been added to the real and imaginary parts of the simulated scattered fields. Normalized standard deviations of 10^{-5}, 10^{-4}, 10^{-3}, 10^{-2}, and 10^{-1} are used in the simulations. The normalized standard deviation mentioned earlier is defined as the standard deviation of the Gaussian noise divided by the rms value of the scattered fields. Here, the signal-to-noise ratio (SNR) is inversely proportional to the normalized standard deviation. The numerical result for this example is plotted in Fig. 4. It is understood that the effect of noise is negligible for normalized standard deviations below 10^{-3}.

In the second example, we selected the peanut shape function $F(\theta) = (0.026 + 0.009 \cos 2\theta)$ m with silver material (i.e., $\sigma = 6.17 \times 10^7$ s/m). The purpose of this example is to show that our method is able to reconstruct a scatter whose shape function has two concavities. Satisfactory results are shown in Fig. 5.

In the third example, the shape function is selected to be $F(\theta) = (0.02 + 0.004 \sin 2\theta + 0.008 \sin 3\theta)$ m, where copper material is selected (i.e., $\sigma = 5.8 \times 10^7$ s/m). Note that the shape function is not symmetrical about either the x– and y-axis. This example has further verified the reliability of our algorithm. Refer to Fig. 6 for details.

IV. Conclusions

In this paper, we have presented a study of applying the GA to reconstruct the shape and conductivity of a metallic object through knowledge of a scattered field. Based on the boundary condition and measured scattered field, we have derived a set of nonlinear integral equations and reformulated the imaging problem into an optimization problem. By using the GA, the shape and conductivity of the object can be reconstructed. Even when the initial guess is far from exact, the GA converges to a global extreme of the cost function, while the gradient-based methods often get stuck in a local extreme. Good reconstruction has been obtained from the scattered fields both with and without the additive Gaussian noise. Numerical results also illustrate that the conductivity is more sensitive to noise than the shape function is. According to our experience, the main difficulties in applying the GA to this problem are how to choose the parameters, such as the population size (M), bit length of the string (L), crossover probability (p_c), and mutation probability (p_m). Different parameter sets will affect the speed of convergence, as well as the computing time required. From the numerical simulation, it is concluded that a population size from 300 to 600, a string length from 8 to 16 bits, and a p_c and p_m in the ranges of $0.7 < p_c < 0.9$ and $0.0005 < p_m < 0.05$ are suitable for imaging problems of this type.

References

[1] A. Roger, "Newton–Kantorovitch algorithm applied to an electromagnetic inverse problem," *IEEE Trans. Antennas Propagat.*, vol. AP-29, pp. 232–238, Feb. 1981.

[2] W. Tobocman, "Inverse acoustic wave scattering in two dimensions from impenetrable targets," *Inverse Problems*, vol. 5, pp. 1131–1144, Dec. 1989.

[3] C. C. Chiu and Y. W. Kiang, "Electromagnetic imaging for an imperfectly conducting cylinders," *IEEE Trans. Microwave Theory Tech.*, vol. 39, pp. 1632–1639, Sept. 1991.

[4] G. P. Otto and W. C. Chew, "Microwave inverse scattering-local shape function imaging for improved resolution of strong scatterers," *IEEE Trans. Microwave Theory Tech.*, vol. 42, pp. 137–141, Jan. 1994.

[5] D. Colton and P. Monk, "A novel method for solving the inverse scattering problem for time-harmonic acoustic waves in the resonance region II," *SIAM J. Appl. Math.*, vol. 46, pp. 506–523, June 1986.

[6] A. Kirsch, R. Kress, P. Monk, and A. Zinn, "Two methods for solving the inverse acoustic scattering problem," *Inverse Problems*, vol. 4, pp. 749–770, Aug. 1988.

[7] F. Hettlich, "Two methods for solving an inverse conductive scattering problem," *Inverse Problems*, vol. 10, pp. 375–385, 1994.

[8] R. E. Kleinman and P. M. van den Berg, "Two-dimensional location and shape reconstruction," *Radio Sci.*, vol. 29, pp. 1157–1169, July/Aug. 1994.

[9] C. C. Chiu and P. T. Liu, "Image reconstruction of a perfectly conducting cylinder by the genetic algorithm," *Proc. Inst. Elect. Eng.*, vol. 143, pp. 249–253, June 1996.

[10] Z. Q. Meng, T. Takenaka, and T. Tanaka, "Image reconstruction of two-dimensional impenetrable objects using genetic algorithm," *J. Electromag. Waves Applicat.*, vol. 13, pp. 95–118, 1999.

[11] F. Xiao and H. Yabe, "Microwave imaging of perfectly conducting cylinders from real data by micro genetic algorithm coupled with deterministic method," *IEICE Trans. Electron.*, vol. E81-C, pp. 784–1792, Dec. 1998.

[12] D. E. Goldgerg, *Genetic Algorithm in Search, Optimization and Machine Learning*. Reading, MA: Addison-Wesley, 1989.

[13] F. M. Tesche, "On the inclusion of loss in time domain solutions of electromagnetic interaction problems," *IEEE Trans. Electromagn. Compat.*, vol. 32, pp. 1–4, Feb. 1990.

[14] E. C. Jordan and K. G. Balmain, *Electromagnetic Waves and Radiating Systems*. Englewood Cliffs, NJ: Prentice-Hall, 1968.

[15] R. F. Harrington, *Field Computation by Moment Methods*. New York: Macmillan, 1968.

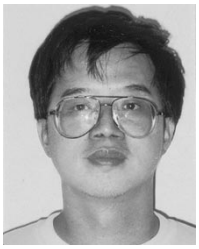

Chien-Ching Chiu was born in Taoyuan, Taiwan, R.O.C., on January 23, 1963. He received the B.S.C.E. degree from the National Chiao Tung University, Hsinchu, Taiwan, R.O.C., in 1985, and the M.S.E.E. and Ph.D. degrees from the National Taiwan University, Taipei, Taiwan, R.O.C., in 1987 and 1991, respectively.

From 1987 to 1989, he served in the ROC Army Force as a Communication Officer. In 1992, he joined the Faculty of the Department of Electrical Engineering, Tamkang University, Taiwan, R.O.C., where he is currently a Professor. From 1998 to 1999, he was a Visiting Scholar at the Massachusetts Institute of Technology, Cambridge, and the University of Illinois at Urbana-Champaign. His current research interests include microwave imaging, numerical techniques in electromagnetics, and indoor wireless communications.

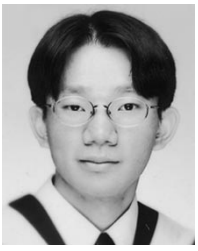

Wei-Ting Chen was born in Hsinchu, Taiwan, R.O.C., on January 9, 1976. He is currently working toward the M.S. degree in electrical engineering at Tamkang University, Taiwan, R.O.C.

His current research interests include numerical techniques in electromagnetics and indoor wireless communications.